Biogeosciences Discuss., 12, 10579–10619, 2015
www.biogeosciences-discuss.net/12/10579/2015/
doi:10.5194/bgd-12-10579-2015

Biogeosciences
Discussions
Open Access

The organic sea surface microlayer in the upwelling region off Peru and implications for air–sea exchange processes

A. Engel and L. Galgani

GEOMAR – Helmholtz Centre for Ocean Research Kiel, Düsternbrooker Weg 20, 24105 Kiel, Germany

Received: 29 May 2015 – Accepted: 03 June 2015 – Published: 09 July 2015

Correspondence to: A. Engel (aengel@geomar.de)

Published by Copernicus Publications on behalf of the European Geosciences Union.

Abstract

The sea surface microlayer (SML) is at the very surface of the ocean, linking the hydrosphere with the atmosphere, and central to a range of global biogeochemical and climate-related processes. The presence and enrichment of organic compounds in the SML have been suggested to influence air–sea gas exchange processes as well as the emission of primary organic aerosols. Among these organic compounds, primarily of plankton origin, are dissolved exopolymers, specifically polysaccharides and proteins, and gel particles, such as Transparent Exopolymer Particles (TEP) and Coomassie Stainable Particles (CSP). These organic substances often accumulate in the surface ocean when plankton productivity is high. Here, we report results obtained in December 2012 during the SOPRAN Meteor 91 cruise to the highly productive, coastal upwelling regime off Peru. Samples were collected from the SML and from ~ 20 cm below, and were analyzed for polysaccharidic and proteinaceous compounds, gel particles, total and dissolved organic carbon, bacterial and phytoplankton abundance. Our study provides insight to the physical and biological control of organic matter enrichment in the SML, and discusses the potential role of organic matter in the SML for air–sea exchange processes.

1 Introduction

The sea-surface microlayer (SML) is the uppermost layer of the water-column and the interface between the ocean and the atmosphere. The accumulation of organic matter, distinct physical and chemical properties and a specific organismal community (neuston) distinguish the SML as a unique biogeochemical and ecological system. It has been suggested that the SML has a gel-like nature (Cunliffe and Murrell, 2009) of varying thickness with dissolved polymeric carbohydrates and amino acids present as well as gel particles, such as Transparent Exopolymer Particles (TEP) of polysaccharidic composition, and Coomassie Stainable Particles (CSP) of proteinaceous com-

BGD
12, 10579–10619, 2015

The organic sea surface microlayer in the upwelling region

A. Engel and L. Galgani

Title Page
Abstract | Introduction
Conclusions | References
Tables | Figures
◀◀ | ▶▶
◀ | ▶
Back | Close
Full Screen / Esc
Printer-friendly Version
Interactive Discussion

position. These compounds originate from high molecular weight polymers that are released form phytoplankton and bacterial cells by exudation and cell break up (Chin et al., 1998; Engel et al., 2004; Verdugo et al., 2004). Polysaccharide-rich gels, known as transparent exopolymer particles (TEP), were attributed mainly to phytoplankton exudation (Passow, 2002), while the production of protein-containing gels, such as coomassie stainable particles (CSP) has been related to cell lysis and decomposition, as well as to the absorption of proteins onto non-proteinaceous particles (Long and Azam, 1996). Gels are transported to the SML by rising bubbles (Azetsu-Scott and Passow, 2004; Zhou et al., 1998) or are produced from dissolved precursors directly at the air–sea interface during surface wave action (Wurl et al., 2011). Gel particles can promote microbial biofilm formation (Bar-Zeev et al., 2012) and mediate vertical organic matter transport, either to the atmosphere (Leck and Bigg, 2005; Orellana et al., 2011) or to the deep ocean (Passow, 2002).

Accumulation of organic matter in the SML may be tightly coupled to phytoplankton dynamics in the water-column (Bigg et al., 2004; Gao et al., 2012; Matrai et al., 2008; Galgani et al., 2014). Thus, organic matter accumulation and composition in the SML may also reflect the sensitivity of marine microorganisms in the surface ocean to environmental changes, which was shown during previous mesocosms studies (Engel et al., 2013; Riebesell et al., 2009; Schulz et al., 2013). Processes determining organic matter accumulation and compositional changes in the SML may be relevant for two main processes that occur at the air–sea interface and are important to understand oceanic feedback on atmospheric dynamics: sea-spray aerosol (SSA) emission and composition and air–sea gas exchange processes. During biologically productive periods, a high amount of SSA with a predominant organic composition is emitted from the ocean's surface (O'Dowd et al., 2004). These compounds primarily reveal a polysaccharidic gel-like composition, suggesting that the abundance and size of dissolved polysaccharides and marine gels in the sea surface may influence the organic fraction of SSA (Orellana et al., 2011; Russell et al., 2010). It has also been shown that the presence of surface active substances (surfactants) in the sea-surface microlayer, like biogenic material as polysaccharides and amino acids, leads to capillary wave damping and alters the molecular diffusion of gases (Frew et al., 1990; Liss and Duce, 2005) and therewith affects gas exchange rates particularly at lower wind speed (Jähne and Haußecker, 1998). In this respect, the understanding of sources, composition and fate of biological components in the surface layer of the ocean becomes of particular relevance for environments where biological productivity is high, like in coastal upwelling regimes.

The upwelling coastal region off Peru extends between 4 and about 40° S. In this area, upwelling processes are sustained by winds all along the year but feature high inter-annual ecosystem variability induced by the El Niño–Southern Oscillation (ENSO) cycle (Tarazona and Arntz, 2001). Eastern Boundary Upwelling Systems (EBUS) like the system off Peru are characterized by high biological productivity supported by deep-upwelling of nutrients and often associated with subsurface Oxygen Minimum Zones (OMZs). The supply of oxygen to the OMZ is largely controlled by physical, i.e. diffusive and advective, mechanisms, whereas biological processes, i.e. respiration of organic matter, provide sinks (Lachkar and Gruber, 2011). OMZs are significant source regions for major climate relevant gases such as carbon dioxide, methane, hydrogen sulfide and nitrous oxide (Paulmier et al., 2008, 2011). Processes affecting gas exchange in these regions need to be understood in order to accurately estimate trace gas fluxes from the ocean to the atmosphere and consequences on climate.

During the SOPRAN cruise Meteor91 (M91), we drove our attention to organic matter components at the surface since properties of the SML may represent a major uncertainty for gas, heat and aerosol fluxes in this region. During our cruise, organic matter concentration and composition of the SML and the underlying seawater was studied on 39 different stations, providing the most extensive data-set the SML in EBUS so far.

2 Material and methods

2.1 Field information and sampling

The R/V Meteor cruise M91 studied the upwelling region off Peru (Bange, 2013). Samples were collected between 4.59° S and 82.0° W, and 15.4° S and 77.5° W from 3 to 23 December in 2012. The overall goal of M91 was to conduct an integrated biogeochemical study on the upwelling region off Peru in order to assess the importance of oxygen minimum zones (OMZs) for the sea–air exchange of various climate-relevant trace gases and tropospheric chemistry.

On 37 different stations between 5 and 16° S off the Peruvian coast (Fig. 1), a total of 39 SML samples was collected from a rubber boat using a glass plate sampler according to the original approach described by Harvey and Burzell (1972). Two stations were sampled twice in a time frame of 24 h (stations 12_1 and 12_3, 16_2 and 16_3). Our glass plate with the dimensions of 500 mm (length) × 250 mm (width) × 5 mm (thickness) was made of silicate glass and had an effective sampling surface area of 2000 cm^2 (considering both sides). For each sample, the glass plate was inserted into the water perpendicular to the surface and withdrawn at a controlled rate of $\sim 20\,\text{cm}\,\text{s}^{-1}$. The sample, retained on the glass because of surface tension, was removed with the help of a Teflon wiper. Samples were collected against wind direction to avoid contamination with the rubber boat and for each sample the glass plate was dipped and wiped about twenty times. The exact number of dips and the total volume collected were recorded. Samples were collected into acid cleaned (HCl, 10 %) and Milli-Q washed glass bottles, and the first milliliters were discarded and used to rinse the bottles. Prior to each sampling, both glass plate and wiper were washed with HCl (10 %) and intensively rinsed with Milli-Q water. At the sampling site, both instruments were copiously rinsed with seawater in order to minimize any possible contamination with alien material while handling or transporting the devices.

The SML thickness (d, m) was estimated as follows:

$$d = V/(A \times n) \tag{1}$$

Where V is the SML volume collected, i.e. 60–140 mL, A is the sampling area of the glass plate ($A = 2000\,\mathrm{cm}^2$) and n is the number of dips.

At the same stations, after sampling the SML about 500 mL samples from the underlying seawater (ULW) were collected at ~ 20 cm depth by holding an acid cleaned (HCl 10 %) and Milli-Q rinsed glass bottle. For safety reasons sampling for the SML from a rubber boat could be made only during daylight hours.

2.2 Chemical and biological analyses

2.2.1 Total organic carbon (TOC) and dissolved organic carbon (DOC)

Samples for TOC and DOC (20 mL) were collected in to combusted glass ampoules, DOC after filtration through combusted GF/F filters (8 h, 500 °C). Samples were acidified with 80 µL of 85 % phosphoric acid, heat sealed immediately, and stored at 4 °C in the dark until analysis. DOC and TOC samples were analyzed by applying the high-temperature catalytic oxidation method (TOC -VCSH, Shimadzu) after Sugimura and Suzuki (1988). The instrument was calibrated every 8–10 days by measuring standard solutions of 0, 500, 1000, 1500, 2500 and 5000 $\mu\mathrm{g\,C\,L}^{-1}$, prepared from a potassium hydrogen phthalate standard (Merck 109017). Every measurement day, ultrapure (MilliQ) water was used for setting the instrument baseline, followed by the measurement of deep-sea water with known DOC/TOC concentration (Dennis Hansell, RSMAS, University of Miami) to verify results. Additionally, two internal standards with DOC within the range of those in samples were prepared each measurement day using a potassium hydrogen phthalate (Merck 109017). DOC and TOC concentration was determined in each sample from 5 to 8 injections. Particulate organic carbon (POC) was determined as the difference between TOC and DOC.

2.2.2 Total nitrogen (TN) and total dissolved nitrogen (TDN)

TN and TDN were determined simultaneously with TOC and DOC, respectively, using the TNM-1 detector on the Shimadzu analyzer. Nitrogen in the samples is combusted and converted to NO$_x$, which chemiluminesces when mixed with ozone and can be detected using a photomultiplier (Dickson et al., 2007). Calibration of the instrument was done every 8–10 days by measuring standard solutions of 0, 100, 250, 500 and 800 µg N L^{-1}, prepared with potassium nitrate Suprapur® (Merck 105065). Particulate nitrogen (PN) was determined as the difference between TN and TDN.

2.2.3 Total, dissolved and free amino acids

For total hydrolysable amino acids (THAA), 5 mL of sample were filled into pre-combusted glass vials (8 h, 500 °C) and stored at −20 °C until analysis. Samples for dissolved hydrolysable (DHAA) and free amino acids (FAA) were additionally filtered through 0.45 µm Millipore Acrodisc® syringe filters and then stored in the same way as samples for THAA. Analysis was performed according to Lindroth and Mopper (1979) and Dittmar et al. (2009) with some modifications. Duplicate samples were hydrolyzed for 20 h at 100 °C with hydrochloric acid (suprapur, Merck) and neutralized by acid evaporation under vacuum in a microwave at 60 °C. Samples were washed with water to remove remaining acid.

Analysis was performed on a 1260 HPLC system (Agilent). Thirteen different amino acids were separated with a C^{18} column (Phenomenex Kinetex, 2.6 µm, 150 × 4.6 mm) after in-line derivatization with o-phtaldialdehyde and mercaptoethanol. Solvent A was 5 % acetonitrile (LiChrosolv, Merck, HPLC gradient grade) in sodiumdihydrogen-phospate (Merck, suprapur) buffer (PH 7.0), Solvent B was acetonitrile. A gradient was run from 100 % solvent A to 78 % solvent A in 50 min. FAA were determined from DHAA samples without prior hydrolysis in separate analyses. Particulate hydrolysable amino acids (PHAA) were determined by subtracting DHAA from THAA.

2.2.4 Total and dissolved combined carbohydrates

For total and dissolved hydrolysable carbohydrates > 1 kDa (THCHO and DHCHO), 20 mL were filled into pre-combusted glass vials (8 h, 500 °C) and kept frozen at −20 °C until analysis. Samples for DHCHO were additionally filtered through 0.45 µm Millipore Acrodisc® syringe filters. The analysis was conducted according to Engel and Händel (2011) applying HPAEC-PAD on a Dionex ICS 3000. Samples were desalinated by membrane dialysis (1 kDa MWCO, Spectra Por) for 5 h at 1 °C, hydrolyzed for 20 h at 100 °C with 0.8 M HCl final concentration, and neutralized through acid evaporation (N_2, 5 h, 50 °C) Two replicate samples were analyzed. Particulate hydrolysable carbohydrates (PHCHO) were determined as the difference between THCHO and DHCHO.

2.2.5 Gel particles

Total area, particle numbers and equivalent spherical diameter (d_p) of gel particles were determined by microscopy after Engel (2009). Therefore, 20 to 30 mL were filtered onto 0.4 µm Nuclepore membranes (Whatmann) and stained with 1 mL Alcian Blue solution for polysaccharidic gels, i.e. transparent exopolymer particles (TEP), and 1 mL Coomassie Brilliant Blue G (CBBG) working solution for proteinaceous gels, i.e. Coomassie Stainable Particles (CSP). Filters were mounted onto Cytoclear© slides and stored at −20 °C until microscopy analysis.

The size-frequency distribution of polysaccharidic and proteinaceous gels was described by:

$$\frac{\mathrm{d}N}{\mathrm{d}(d_\mathrm{p})} = k d_\mathrm{p}^{\delta} \tag{2}$$

where dN is the number of particles per unit water volume in the size range d_p to ($d_p + \mathrm{d}(d_p)$) (Mari and Kiørboe, 1996). The factor k is a constant that depends on the total number of particles per volume, and δ ($\delta < 0$) describes the spectral slope of the size distribution. The value δ is related to the slope of the cumulative size distribution

$N = ad_p^{\beta}$ by $\delta = \beta + 1$. The less negative is δ, the greater is the fraction of larger gels. Both δ and k were derived from regressions of $\log(dN/d(d_p))$ vs. $\log(d_p)$. To determine δ, data for CSP and TEP were fitted over the size range 1.05–14.14 µm ESD.

The fractal dimension (D1) was calculated based on δ of the semi-empirical relationship (Burd and Jackson, unpublished data, as referred to in Mari and Burd, 1998 and as applied for TEP also by Harlay et al., 2009):

$$\mathrm{D1} = \frac{(64 - \delta)}{26.2} \tag{3}$$

2.2.6 Heterotrophic bacteria

For bacterial cell numbers, 4 mL samples were fixed with 200 µL glutaraldehyde (25 % final concentration) and stored at −20 °C until enumeration. Samples were stained with SYBR Green I (Molecular Probes). Heterotrophic bacteria were enumerated using a flow cytometer (Becton & Dickinson FACScalibur) equipped with a laser emitting at 488 nm and detected by their signature in a plot of side scatter (SSC) vs. green fluorescence (FL1). Yellow-green latex beads (Polysciences, 0.5 µm) were used as internal standard.

2.2.7 Phytoplankton

For autotrophic cell numbers, 4 mL samples were fixed with 20 µL glutaraldehyde (25 % final concentration), and stored at −80 °C until enumeration. Phytoplankton counts were performed with a FACSCalibur flow-cytometer (Becton Dickinson) equipped with an air-cooled laser providing 15 mW at 488 nm and with a standard filter set-up. The cells were analyzed at high flow rate (∼ 39–41 µL min^{-1}) with the addition of 1 µm-fluorescent beads (Trucount, BD). Autotrophic groups were discriminated on the basis of their forward or right angle light scatter (FALS, RALS) as well as from chlorophyll and phycoerythrin (characteristic for cyanobacterial, mainly *Synechococcus* populations) fluorescence. Cell counts were analyzed using BD CellQuest Pro-Software.

2.2.8 Data analysis

The relative concentration of a substance A in the SML was compared to the underlying water (ULW) by the enrichment factor (EF), defined by:

$$\mathrm{EF} = (A)_{\mathrm{SML}}/(A)_{\mathrm{ULW}} \tag{4}$$

Where (A) is the concentration of a given parameter in the SML or ULW, respectively (GESAMP, 1995). Because the concentration of a component is normalized to its values in the underlying water, EF for different components can be readily compared. Enrichment of a component is indicated by $\mathrm{EF} > 1$, depletion by $\mathrm{EF} < 1$.

Differences in data as revealed by statistical tests (t test) were accepted as significant for $p < 0.05$. Average values for total concentrations are given by their arithmetic mean, averages for ratios by their geometric mean. Calculations, statistical tests and illustration of the data were performed with the software packages Microsoft Office Excel 2010, Sigma Plot 12.0 (Systat) and Ocean Data View (Schlitzer, 2013). Average values are reported with ±1 standard deviation.

3 Results

3.1 The physical environment

Coastal upwelling of deep water resulted in strong gradients of surface seawater temperature and salinity along the Peruvian shelf as well as with increasing distance to the shelf during M91. Salinity measured at about 1 m depth corresponding to the ship's keel varied between 32 and 35 psu with the lowest values occurring close to the coast at stations 10_1 to 10_4, 14_1 and 14_2 and 15_1 to 15_3. Here, temperatures below average (< 19 °C) were recorded indicating the colder, upwelling deep water (Table 1, Fig. 2). Wind speed encountered during the cruise ranged between 0.6 and 9.0 $\mathrm{m\,s^{-1}}$ with the lower wind speeds also observed closer to the coast, i.e. between 12 and

14° S and at the northern stations (Fig. 2). Thus, higher wind speed was observed at the more off-shore stations having higher surface water temperatures, leading to significant co-variation between surface water temperature and wind speed (Fig. 3). Global radiation and UV radiation varied between 10 and 1103 $\mathrm{W\,m^{-2}}$, and between 0.8 and 71 $\mathrm{W\,m^{-2}}$ (data from shipboard measurements on R/V Meteor were retrieved from DSHIP software) with no significant impact of SML organic matter accumulation.

3.2 Organic matter in the SML

The thickness of the SML calculated from glass plate sampling during this cruise ranged between 45 and 60 µm, with an overall mean value of 49 ± 8.9 µm ($n = 39$). This value is in good accordance with previous observations for the SML when sampled with a glass plate (Cunliffe et al., 2011, 2013).

In general, concentration of organic components in the SML showed spatial distribution patterns resembling those of temperature and wind speed (compare Figs. 3–5); highest values for nearly all components were observed at the upwelling stations 10_1 to 10_4, 14_1 and 14_2 and 15_1 to 15_3 (Fig. 1).

Unless stated otherwise, all observations described in this paragraph relate to the SML.

Phytoneuston abundances ranged between 3.7×10^3 and 1.9×10^5 $\mathrm{mL^{-1}}$ for cyanobacteria (mainly *Synechococcus spp.*) and between 5.4×10^3 and 3.0×10^5 $\mathrm{mL^{-1}}$ for other pico- and nanoautotrophs. Generally highest abundance of nano- and picoautotrophs in the SML was determined on and close to the upwelling stations (Fig. 4). On all other stations, cell abundance of cyanobacteria and phytoplankton differed spatially, with higher abundance of phytoeukaryotes at the southern stations and higher numbers of cyanobacteria at the northern stations (Fig. 4). Heterotrophic bacteria were determined in abundances between 3.0×10^4 and 8.5×10^6 $\mathrm{mL^{-1}}$ with highest numbers observed at the upwelling stations and southeast of the upwelling (Fig. 4).

TOC concentration ranged between 82 and 199 $\mathrm{\mu mol\,L^{-1}}$, and was clearly higher than DOC concentration on all stations. Particulate Organic Carbon (POC) concentration was calculated as the difference between TOC and DOC and ranged between 2.3 to 96 µmol L^{-1}. Highest POC concentration was observed at the upwelling stations (Fig. 5). In general, POC concentration was highly inversely correlated to temperature ($r = -0.67$, $p < 0.001$) and to wind speed ($r = -0.48$, $p < 0.001$) (Table 3). DOC concentration ranged between 71 and 122 µmol L^{-1} (Table 2) and, in contrast to POC, was not significantly related to temperature or wind speed (Table 3). Relatively high DOC concentrations of about 100 µmol L^{-1} were observed at stations 9 and 9_2 (Fig. 5), but excluding these stations from analysis did not reveal a correlation to temperature or wind speed either. DOC is a bulk measure and is quantitatively dominated by refractory compounds that are independent from recent biological productivity. More closely linked to productivity and likely stimulated by the upwelling of nutrients along the Peruvian coast are labile and semi-labile compounds such as dissolved combined carbohydrates and amino acids. Indeed, both DHCHO and DHAA reached highest concentrations at the upwelling stations (Fig. 5). Thereby, maximum concentration of DHCHO of 2668 nmol L^{-1} (mean: 1111 ± 550 nmol L^{-1}) was observed at station 15_2, slightly south of the station 14_1 exhibiting highest DHAA concentrations of 2017 nmol L^{-1} (mean: 770 ± 359 nmol L^{-1}) (Table 2). In general high DHCHO concentration was more focused to the upwelling, and exhibited strong horizontal gradients to the northern and southern stations.

DHHA concentration was on average lower than DHCHO concentration (Table 2) and horizontal differences were less pronounced than for DHCHO. Both components of semi-labile DOC were inversely correlated to temperature (DHCHO $r = -0.44$, $n = 39$, $p < 0.001$; DHAA: $r = -0.47$, $n = 30$, $p < 0.001$), linking their accumulation in the SML to productivity in the cold upwelling waters.

Concentrations of combined carbohydrates and amino acids in particles and in gels (TEP, CSP) in particular were highest at the coastal upwelling stations also. Particulate carbohydrates and amino acids (PHCHO, PHAA) were highly correlated to POC concentrations (PHCHO $r = 0.70$, $n = 39$, $p < 0.001$; PHAA: $r = 0.81$, $n = 30$, $p < 0.001$). In contrast to the dissolved components, particles contained on average higher concentrations of amino acids compared to carbohydrates (Table 2), indicating a more rapid loss of DHAA after release from particles.

In general, CSP were more abundant than TEP (Table 2), but variability of gel particles abundance was high, yielding lowest values of total TEP area of 6.9 $\mathrm{mm^2\,L^{-1}}$ at station 13_1 and highest values of 408 $\mathrm{mm^2\,L^{-1}}$ at station 15_1, about 100 nautical miles apart. Although highest abundance of both TEP and CSP were observed close to the coastal upwelling, apart from this area distribution of TEP in the SML clearly differed from that of CSP (Fig. 5). While higher TEP abundance was observed at the northern stations, CSP abundance was more pronounced at the southern stations. Moreover, stations of highest and lower concentration of CSP were different from those of TEP. Lowest value of CSP total area of 137 $\mathrm{mm^2\,L^{-1}}$ was observed at station 11_1 and highest value of 3051 $\mathrm{mm^2\,L^{-1}}$ at station 14_1.

3.3 Accumulation patterns in the SML

For almost all components investigated during this study, concentration in the SML was significantly related to the respective concentration in the ULW (Table 3). Thereby, correlations between SML and ULW were strongest for combined carbohydrates, particularly for DHCHO. Close correlations were also observed for bulk organic carbon measurements, i.e. TOC, DOC, and derived therefrom POC. For dissolved nitrogenous compounds, i.e. TDN, FAA and DHAA no relationship between SML and ULW concentrations were observed, suggesting that loss or gain of these compounds in the SML were faster than exchange processes with the ULW. Temperature had an effect on most organic compounds in the SML, with generally higher concentrations at lower temperature (Table 3). Concentrations of particulate components POC, TEP, PHCHO, PHAA and particulate nitrogen (PN) were also inversely related to wind speed, whereas DHCHO and DHAA were inversely related to temperature but not to wind speed. Clear differences were observed for the two different gel particle types determined in this study. In contrast to TEP, neither abundance nor total area of CSP were related to wind speed, nor to seawater temperature. Instead abundance of CSP in the SML was mostly related to their abundance in ULW. However, with the exception of CSP, particulate components in the SML were affected by changes in wind speed more than concentration of dissolved compounds (Table 3).

Enrichment factors indicated a general accumulation of organic matter in the SML with respect to the underlying seawater (ULW) (Fig. 6), which happened at most stations. Thereby, clear differences were observed between EF values of different components. The highest enrichment was observed for free amino acids (FAA) that were enriched more than 10-fold at some stations. Moreover, FAA were consistently enriched in the SML, except for one station where the lowest FAA concentration was determined ($49\,\mathrm{nmol\,L^{-1}}$).The largest variability of EF was observed for abundance and total area of gel particles. For TEP total area, values of EF ranged between 0.2–12, with highest EF observed at the coastal upwelling station 14_1, where the wind speed recorded was $0.6\,\mathrm{m\,s^{-1}}$. In proximity of this station, the lowest EF of TEP was determined (station 15_3) indicating a clear depletion at wind speed of $7\,\mathrm{m\,s^{-1}}$. The EF of CSP total area ranged between 0.4 and 4.8. Thus highest EF of CSP was clearly lower than for TEP, and in contrast to TEP it was observed at the more offshore station 18_2 at a higher wind speed rate of $9.2\,\mathrm{m\,s^{-1}}$. For TEP as well as for CSP median EF varied around a value of one, suggesting that marine gel accumulation is spatially highly variable, and in our cruise marine gels did not generally become enriched in the SML. Total and dissolved hydrolysable amino acids (THAA, DHAA) were enriched in the SML at almost all stations (Fig. 6), with EF of 0.8–4.6 (DHAA) and 0.4–3.4 (THAA). Median EFs were 1.7 and 1.4 for DHAA and THAA, respectively. Total and dissolved hydrolysable carbohydrates (THCHO, DHCHO) concentrations in the SML were often similar to the ULW, with EF values ranging between 0.6 and 1.4 (DHCHO) and between 0.3 and 1.7 (THCHO), respectively. In contrast to all other organic chemical compounds, bacteria were found to be depleted in the SML at almost all stations (Fig. 6), having a median EF of 0.8. Variability of EF was generally smaller for dissolved components than for particulates, suggesting again differences in the accumulation dynamics.

Title Page
Abstract Introduction
Conclusions References
Tables Figures
◀◀ ▶▶
◀ ▶
Back Close
Full Screen / Esc
Printer-friendly Version
Interactive Discussion

3.4 Size distribution of gel particles within the SML

Abundance of polysaccharidic gel particles, i.e. TEP, decreased with increasing size according to the power law function given in Eq. (1) (Fig. 7). The slope, δ, of the size spectrum varied between −2.63 and −1.38, revealing an average fractal scaling exponent of TEP in the SML of $D1 = 2.51 \pm 0.010$. This value is close to 2.55 proposed by Mari and Burd (1998) for seawater TEP.

The number of TEP in the smallest size class (1.25–1.77 µm) ranged from 96 to 1.38×10^4 mL^{-1}, while for CSP, variability of abundance in the 1.25–1.77 µm size class was much smaller and ranged between 1.46×10^4 and 2.33×10^5 mL^{-1}, suggesting that proteinaceous particles represent the largest fraction of small gel particles. Similar to TEP, size distribution of CSP followed the power law relationship of Eq. (2), yielding δ values between −1.12 and −2.01. With a D1 value of 2.50 ± 0.008 the fractal dimension of CSP was almost identical to that of TEP.

No overall relationship was established between the slope of the size distribution of TEP and wind velocity (δTEP vs. wind speed: $r = -0.19$, $n = 39$, $p = 0.20$). However, TEP size distribution was much steeper at the station with highest wind speed compared to the one with lowest wind velocity (δTEP at 0.6 m s^{-1} = −1.51, $r^2 = 0.95$, $n = 7$; δTEP at 9.0 m s^{-1} = −2.31, $r^2 = 0.95$, $n = 7$) (Fig. 8a). In particular, at the high wind speed a loss of larger TEP, i.e. > 7 µm was observed in the SML compared to the ULW and relative to the low wind speed station.

For CSP a significant inverse relationship was observed between the slope δ and wind speed (δCSP vs. wind speed: $r = -0.61$, $n = 37$, $p < 0.001$). A loss of larger CSP was also observed by direct comparison between low and high wind speed stations (Fig. 8b). But here, CSP > 7 µm were rather increased in the SML at low wind speed compared to the ULW and to the high wind speed stations (δCSP at 0.6 m s^{-1} = −1.12, $r^2 = 0.92$, $n = 7$; δTEP at 9.0 m s^{-1} = −1.45, $r^2 = 0.97$, $n = 7$).

4 Discussion

It has been suggested that the presence of organic matter in the SML influences a series of processes relevant to air–sea exchange of gases, dissolved and particulate components. EBUS are characterized by high biological productivity and strong across shelf gradients of organic matter concentration. Therefore EBUS are ideal model systems to study the linkages of biological productivity and SML properties, with respect to characteristics of organic matter composition and factors controlling organic matter enrichment in the SML.

4.1 Organic matter characteristics of the SML

Strong horizontal gradients in organic matter concentration of the SML were observed for the coastal and shelf-break region off Peru with generally higher organic matter concentrations in the SML towards the area of upwelling of colder, nutrient-rich deep water. Hence, increasing ecosystem productivity is one likely factor responsible for higher concentrations of organic components in the SML. Significant correlations of organic matter concentrations in the SML and ULW were determined and showed that the SML basically reflects the underlying seawater system. The close connectivity between microlayer organic properties and biological development was also shown during a recent mesocosm study, indicating that ecosystem changes impact microlayer organic matter composition and concentration (Galgani et al., 2014). Despite this finding that relates to a more general characteristic of the SML, clear differences in the accumulation behavior of different organic matter components were determined during this study and are in good accordance with previous observations. A generally higher SML accumulation was observed for amino acids compared to carbohydrates. Significant enrichment of amino acids in the SML has been determined previously for coastal as well as open ocean sites, and higher accumulation of FAA compared to DHAA and THAA, as also observed during this study, appears to be a consistent SML feature (Henrichs and Williams, 1985; Carlucci et al., 1992; Kuznetsova and Lee, 2001, 2002; Kuznetsova et al., 2004; Reinthaler et, al. 2008). As for this study, wind velocity and temperature have not been identified as physical factors responsible for amino acid enrichment in the past (Kuznetsova et al., 2004). FAA and DHAA are labile to semilabile substrates and taken-up by heterotrophic microorganisms (Keil and Kirchman, 1992). Turn-over times of these components in the water column are usually in the range of minutes to days (Fuhrman and Ferguson, 1986; Benner, 2002). The observed accumulation of FAA and DHAA in the SML may therefore be related to a reduced activity of bacteria. For different coastal Baltic Sea sites, Stolle et al. (2010) determined a lowered bacterial biomass production in the SML, despite bacterial cell numbers being similar to those in the ULW. During M91 bacteria were mostly depleted in the SML compared to the ULW supporting the idea of the SML being an "extreme environment" for bacteria. Earlier studies showed that some bacteria may be adapted to UV radiation in the SML as well as in the ULW (Carlucci et al., 1985; Agogue et al., 2005). Amino acid consumption by bacterioneuston under UV-B stress may be reduced (Santos et al., 2012), which may give an explanation for the higher concentrations of FAA and DHAA in the SML during M91. However, no significant correlation between bacterial abundance and UV radiation or between UV radiation and amino acid concentrations in the different pools were observed during this study, suggesting that history rather than instantaneous UV radiation may be responsible for controlling bacteria and organic matter components in the SML.

In addition to ULW properties, wind speed was determined as a factor controlling accumulation of particulate material, in particular TEP, in the SML. TEP are marine gel particles that have been hypothesized to be neutrally or positively buoyant thanks to high water content (Engel and Schartau, 1999; Azetsu-Scott and Passow, 2004). TEP were moreover suggested to form within the SML, either by wind-shear induced aggregation of precursors or due to coalescence of pre-cursor molecules, primarily polysaccharides when entrained air bubbles burst at the sear surface (Wurl et al., 2011). Adsorption of DOM onto bubble surfaces and TEP formation by bubble bursting have been determined during experimental flotation and bubbling studies using surface seawater from different locations (Wallace and Duce, 1978; Zhou et al., 1998). Bubble scavenging of DOM in the upper water column may thus be responsible for high concentrations of TEP at the SML, because more TEP precursors are lifted up the water-column (Wurl et al., 2011; Gao et al., 2012). In addition, compression and dilatation of the SML due to capillary waves may increase the rate of polymer collision, subsequently facilitating gel aggregation (Carlson, 1993). During M91, TEP enrichment in the SML was inversely related to wind speed, supporting earlier observations of Wurl and colleagues (Wurl et al., 2009, 2011). However, in contrast to earlier observations showing EF values > 1 for TEP in the SML also at higher wind speed, we found the SML to be depleted of TEP at wind speed of $\sim 5\,\mathrm{m\,s^{-1}}$ and above. It has been suggested that TEP aggregation rates in the SML are higher than in the ULW, due to enhance collision rates by shear or bubble bursting. TEP have been shown to control coagulation efficiencies of solid particles, such as diatoms and coccolithophores (Logan et al., 1995; Engel, 2000; Chow et al., 2015). At higher wind speed, increased aggregation rates of TEP with solid particles, eventually containing mineral ballast, may thus favor the formation of aggregates that become negatively buoyant and sink out of the SML. This may explain the observed loss of larger TEP ($> 7\,\mu$m) from the SML relative to the ULW and to the SML at low wind speed. Enhanced aggregation rates could then also explain the inverse relationship between POC and wind speed, observed during this study.

In contrast to TEP, no impact of wind speed was determined for CSP accumulation, or for CSP enrichment in the SML. Moreover, clear spatial differences were observed for the distribution of TEP and CSP in the SML. Although both TEP and CSP are gel particles that form from dissolved organic precursors released by microorganisms, their spatial and temporal occurrence in marine systems can be quite different, e.g. TEP accumulate towards the end of phytoplankton blooms while CSP rather co-occur with maximum phytoplankton abundance (Cisternas- Novoa et al., 2015; Engel et al., 2015). Moreover, the depth distribution of TEP and CSP was shown to be different for open ocean sites (Cisternas-Novoa et al., 2015). These spatial and temporal differences in the occurrence of TEP and CSP in the water column may explain the spatial separation of both types of marine gels in the SML observed during this study. However, the observed differences in relation to wind speed suggest that additional factors control the enrichment of TEP and CSP in the SML. It has been shown that CSP are less prone to aggregation than TEP (Prieto et al., 2002; Engel et al., 2015). Similarly, CSP may be less involved in aggregation formation and sinking out of the SML at higher wind speed. Yet, an inverse relationship between the slope of the CSP size distribution in the SML and wind speed was observed during M91, showing larger CSP in the SML at low wind speed. This suggests that CSP as well as TEP may be involved in slick formation that becomes disrupted when wind speed increases.

4.2 Implications of organic matter accumulation in EBUS

4.2.1 Air–sea gas exchange

Although the SML and surface active substances (surfactants) within are widely believed affecting the exchange of gases and heat at the air–sea interface (Davies, 1966; Frew, 1997; Salter et al., 2011), particularly at lower wind speeds (Liss, 1983), we still have little quantitative knowledge on how natural organic components at the immediate sea-surface alter the gas transfer velocity in water (kw). Our data showed a depletion of the SML with respect to TEP and POC at wind speeds $> 5\,\mathrm{m\,s^{-1}}$, suggesting that an effect of these “insoluble” components on gas exchange is, if any, operating only at low wind speed. Due to their fractal scaling, gel particles have a relatively large surface to volume ratio and may act as a cover, reducing molecular diffusion rates at the interface between air and sea.

More independent of wind speed was the accumulation of dissolved organic components in the SML during M91. Dissolved organic matter, like dissolved carbohydrates and amino acids, have demonstrated surfactant properties and reduced gas transfer velocity in water (kw) at low wind speed in laboratory experiments (Goldman et al., 1988; Frew et al., 1990). The reduction of kw is thereby believed to be related to a dampening of small, capillary waves. Salter et al. (2011) recently showed that artificial surfactants can suppress gas transfer velocity by up to 55 % at sea. Suppression of k666 (i.e. kw normalized to a Schmidt number of 666) during their field study was depending on wind speed, but was detected up to 11 $\mathrm{m\,s^{-1}}$, encompassing the full range of wind speed determined during M91. Thus, accumulation of natural organic surfactant as observed during this study may have had an influence on gas exchanges rates as well.

Across the water–air interface, gases of climatic relevance exhibit different behaviors: methane (CH_4) shows a discontinuous concentration while carbon dioxide (CO_2) does not (Upstill-Goddard, 2006). CH_4 diffusivity across the SML has been proposed being mediated by SML bacteria, as possible sink (Upstill-Goddard et al., 2003) or source of this greenhouse gas (Cunliffe et al., 2013). About ~ 30 % of the atmospheric concentration of nitrous oxide (N_2O), one of the strongest greenhouse gases and responsible for ozone depletion, is supported by oceanic sources (Solomon et al., 2007). Of total oceanic N_2O production, oxygen minimum zones (OMZs) contribute about 25–75 % (Bange et al., 2001). In EBUS, high primary production and induced high aerobic remineralization associated with large-scale circulation maintain the presence of OMZs (Gutknecht et al., 2013; Paulmier and Ruiz-Pino, 2009), which, in the last decades, have been expanding and intensifying due to enhanced stratification and reduced ventilation (Keeling et al., 2010; Stramma et al., 2008). Our study was intended to understand how organic matter accumulation in the SML might mediate the transfer rate of trace- and greenhouse gases like N_2O in oceanic regions like OMZs affected by a changing climate. In the case of N_2O, it has recently been shown that it can interact with biological processes specifically by binding to aromatic groups present in certain amino acids like tyrosine and phenilanine (Cao et al., 2014). Tyrosine and phenilanine in the SML of our study represented a small molar percentage of total amino acids pool, with averages in the dissolved fraction (DHAA) of 1.5 ± 0.3 % (tyrosine) and 1.9 ± 0.3 % (phenilanine), and in the total fraction (THAA) of 2.2 ± 0.2 % (tyrosine) and 2.9 ± 0.4 % (phenilanine), but were present. As we found evidence of overall amino acids SML accumulation during our cruise, for those amino acids in particular the median EF both in the total (THAA) and in the dissolved (DHAA) fraction was > 1, suggesting a possible interaction of SML organic components with N_2O in the coastal upwelling region off Peru. In details, median EF for tyrosine was 1.5 (both THAA and DHAA) and for phenilanine we found a median EF = 1.3 (THAA) and EF = 1.7 (DHAA). Amino acids enrichment in the SML has been previously reported (Kuznetsova and Lee, 2002; Kuznetsova et al., 2004; van Pinxteren et al., 2012; Cunliffe et al., 2013; Henrichs and Williams, 1985), and might be due to high surface-active properties because of zwitterionic characteristics of the molecules, probably creating a rather stable layer even at higher wind speeds, thus representing an important barrier for air–sea gas exchange.

Overall, our results showed that accumulation of organic substances occurs in EBUS and is related to the increased productivity. Hence, the organic SML may play a particularly important role for exchange of climate relevant gases that are associated to high organic matter production and resulting anoxia in upwelling systems like the one off Peru.

4.2.2 Organic aerosol production

The structure of sea-spray aerosols (SSA) originating by bubble bursting at the sea surface is a function of biological, chemical and physical properties of the SML, which may comprise a vast array of organic surface-active compounds, microorganisms, and exopolymer gels (Leck and Bigg, 2005; Quinn and Bates, 2011). Despite recent evidences showing that high levels of chlorophyll *a* are not directly related to the organic carbon content of SSA (Quinn et al., 2014), still organic SSA largely derive from the oceanic surface layer and therefore are also subject to the effects of climate change on marine systems (Andreae and Crutzen, 1997). Polysaccharides and polysaccharidic nanogels (Russell et al., 2010; Orellana et al., 2011) as well as particulate amino acids and proteinaceous compounds (Kuznetsova et al., 2005) are present in organic SSA particles. During our cruise we found a distinct behavior of dissolved and particulate compounds, the first being rather enriched in the SML (as also shown by median EF for DOC) but mainly composed of amino acids contributing to an accumulation of proteinaceous material quite independently of the wind speed, as opposed to carbohydrates that had similar concentrations in the SML and ULW. Particulates compounds instead, like TEP and CSP, did not preferentially accumulate in the SML, inferring to other processes determining their production and aggregation dynamics. TEP showed a close inverse relationship to wind speed, being depleted above 5 $\mathrm{m\,s^{-1}}$ while the SML concentration of particulate proteinaceous compounds (CSP) did not. As determined by the slope δ of the size distribution spectra for both TEP and CSP, the less negative is δ, the larger is the fraction of marine gels comprising bigger particles, revealing that CSP were generally larger than TEP. In the light of these observations, these accumulation patterns may suggest a compositional organic matter partitioning in the SML that differently affects the processes at the air–water interface relevant for climate.

In the upwelling region off Peru the wind-driven export of polysaccharidic components to the atmosphere might represent a loss-pathway of these organic compounds from the SML that would then contribute to a larger extent to the organic SSA mass. Instead, amino-acids and proteinaceous compounds are probably more stable at the surface exerting their influence on air–sea gas exchange by capillary wave damping.

This characteristic might be valid for many oceanic regions. EBUS and OMZs are special systems with high level of productivity and degradation rates, so it might be difficult to attribute specific organic sources to the processes controlling air–sea gas exchange and SSA production. However, the accumulation of organic matter in the SML, and the distinct behavior of certain compounds at the water–air interface is certainly an important issue for all exchange processes between the ocean and the atmosphere that in the scenario of anthropogenic climate change needs to be deeply investigated.

Acknowledgements. We thank the captain and crew of R/V *Meteor* during cruise leg M91 for logistic support during sampling, especially help related to the rubber boat operation, as well as H. Bange as chief scientist and all the scientific crew. A great acknowledgement goes to J. Roa for helping with SML sampling on board and for TOC/TN and carbohydrates analysis, respectively. Further technical help was provided by R. Flerus, S. Manandhar and N. Bijma for amino acids and microscopy analysis, as well as T. Klüver for flow-cytometry counts. This work was supported by BMBF project SOPRAN II and III (Surface Ocean Processes in the Anthropocene, 03F0611C-TP01 and 03F0662A-TP2.2).

References

Agogue, H., Joux, F., Obernosterer, I., and Lebaron, P.: Resistance of marine bacterioneuston to solar radiation, Appl. Environ. Microb., 71, 5282–5289, 2005.

Andreae, M. O. and Crutzen, P. J.: Atmospheric aerosols: biogeochemical sources and role in atmospheric chemistry, Science, 276, 1052–1058, doi:10.1126/science.276.5315.1052, 1997.

Azetsu-Scott, K. and Passow, U.: Ascending marine particles: significance of transparent exopolymer particles (TEP) in the upper ocean, Limnol. Oceanogr., 49, 741–748, 2004.

Bange, H. W.: Surface Ocean – Lower Atmosphere Study (SOLAS) in the upwelling region off Peru, Cruise No. M91, 1–26 December 2012, Callao (Peru) – Callao (Peru) Rep., Bremen, Germany, 69 pp.,2013.

Bange, H. W., Rapsomanikis, S., and Andreae, M. O.: Nitrous oxide cycling in the arabian sea, J. Geophys. Res.-Oceans, 106, 1053–1065, doi:10.1029/1999jc000284, 2001.

Bar-Zeev, E., Berman-Frank, I., Girshevitz, O., and Berman, T.: Revised paradigm of aquatic biofilm formation facilitated by microgel transparent exopolymer particles, P. Natl. Acad. Sci. USA, 109, 9119–9124, 2012.

Benner, R.: Chemical composition and reactivity, in: Biogeochemistry of Marine Dissolved Organic Matter, edited by: Hansell, D. A. and Carlson, C., Academic Press, Elsevier Science, 59–90, 2002.

Bigg, K. E., Leck, C., and Tranvik, L.: Particulates of the surface microlayer of open water in the central Arctic Ocean in summer, Mar. Chem., 91, 131–141, 2004.

Cao, Q., Gor, G. Y., Krogh-Jespersen, K., and Khriachtchev, L.: Non-covalent interactions of nitrous oxide with aromatic compounds: spectroscopic and computational evidence for the formation of 1 : 1 complexes, J. Chem. Phys., 140, 144304, doi:10.1063/1.4870516, 2014.

Carlson, D. J.: The early diagenesis of organic matter: reaction at the air–sea interface, in: Organic Geochemistry, edited by: Engel, M. H. and Macko, S. A., Plenum Press, New York, 255–268, 1993.

Carlucci, A. F., Craven, D. B., and Henrichs, S. M.: Surface-film microheterotrophs: amino acid metabolism and solar radiation effects on their activities, Mar. Biol., 85, 13–22, 1985.

Carlucci, A. F., Wolgast, D. M., and Craven, D. B.: Microbial populations in surface films: amino acid dynamics in nearshore and offshore waters off southern california, J. Geophys. Res., 97, 5271–5280, doi:10.1029/91jc02614, 1992.

Chin, W.-C., Orellana, M. V., and Verdugo, P.: Spontaneous assembly of marine dissolved organic matter into polymer gels, Nature, 391, 568–572, 1998.

Chow, J. S., Lee, C., and Engel, A.: The influence of extracellular polysaccharides, growth rate, and free coccoliths on the coagulation efficiency of Emiliania huxleyi, Mar. Chem., doi:10.1016/j.marchem.2015.04.010, in press, 2015.

Cisternas-Novoa, C., Lee, C., and Engel, A.: Transparent exopolymer particles (TEP) and coomassie stainable particles (CSP): differences between their origin and vertical distributions in the ocean, Mar. Chem., doi:10.1016/j.marchem.2015.03.009, in press, 2015.

Cunliffe, M. and Murrell, J. C.: The sea-surface microlayer is a gelatinous biofilm, ISME J., 3, 1001–1003, doi:10.1038/ismej.2009.69, 2009.

Cunliffe, M., Upstill-Goddard, R. C., and Murrell, J. C.: Microbiology of aquatic surface microlayers, FEMS Microbiol. Rev., 35, 233–246, 2011.

Cunliffe, M., Engel, A., Frka, S., Gašparović, B., Guitart, C., Murrell, J. C., Salter, M., Stolle, C., Upstill-Goddard, R., and Wurl, O.: Sea surface microlayers: a unified physicochemical and biological perspective of the air–ocean interface, Prog. Oceanogr., 109, 104–116, 2013.

Davies, J. T.: The effect of surface films in damping eddies at a free surface of a turbulent liquid, P. R. Soc. A, 290, 515–526, doi:10.1098/rspa.1966.0067, 1966.

Dickson, A. G., Sabine, C. L., and Christian, J. R. (Eds.): Guide to best practices for ocean CO_2 measurements, in: PICES Special Publication, 3, 191 pp., 2007.

Dittmar, T., Cherrier, J., and Ludwichowski, K.: The analysis of amino acids in seawater, in: Practical Guidelines for the Analysis of Seawater, edited by: Wurl, O., CRC Press, 67–76, 2009.

Engel, A.: The role of transparent exopolymer particles (TEP) in the increase in apparent particle stickiness (α) during the decline of a diatom bloom, J. Plankton Res., 22, 485–497, 2000.

Engel, A.: Determination of marine gel particles, in: Practical Guidelines for the Analysis of Seawater, edited by: Wurl, O., CRC Press, 2009.

Engel, A. and Händel, N.: A novel protocol for determining the concentration and composition of sugars in particulate and in high molecular weight dissolved organic matter (HMW-DOM) in seawater, Mar. Chem., 127, 180–191, 2011.

Engel, A. and Schartau, M.: Influence of transparent expolymer particles (TEP) on sinking velocity of Nitzschia closterum aggregates, Mar. Ecol.-Prog. Ser., 182, 69–76, doi:10.3354/meps182069, 1999.

Engel, A., Thoms, S., Riebesell, U., Rochelle-Newall, E., and Zondervan, I.: Polysaccharide aggregation as a potential sink of marine dissolved organic carbon, Nature, 428, 929–932, 2004.

Engel, A., Borchard, C., Piontek, J., Schulz, K. G., Riebesell, U., and Bellerby, R.: CO_2 increases ^{14}C primary production in an Arctic plankton community, Biogeosciences, 10, 1291–1308, doi:10.5194/bg-10-1291-2013, 2013.

Engel, A., Borchard, C., Loginova, A., Meyer, J., Hauss, H., and Kiko, R.: Effects of varied nitrate and phosphate supply on polysaccharidic and proteinaceous gel particles production during tropical phytoplankton bloom experiments, Biogeosciences Discuss., 12, 6589–6635, doi:10.5194/bgd-12-6589-2015, 2015.

Frew, N. M.: The role of organic films in air–sea gas exchange, in: The Sea Surface and Global Change, edited by: Liss, P. S. and Duce, R. A., Cambridge University Press, UK, 121–172, 1997.

Frew, N. M., Goldman, J. C., Dennett, M. R., and Johnson, A. S.: Impact of phytoplankton-generated surfactants on air–sea gas exchange, J. Geophys. Res.-Oceans, 95, 3337–3352, doi:10.1029/JC095iC03p03337, 1990.

Fuhrman, J. A. and Ferguson, R. L.: Nanomolar concentrations and rapid turnover of dissolved free amino acids in seawater: agreement between chemical and microbiological measurements, Mar. Ecol.-Prog. Ser., 33, 237–242, 1986.

Galgani, L., Stolle, C., Endres, S., Schulz, K. G., and Engel, A.: Effects of ocean acidification on the biogenic composition of the sea-surface microlayer: results from a mesocosm study, J. Geophys. Res.-Oceans, 119, 7911–7924, 2014.

Gao, Q., Leck, C., Rauschenberg, C., and Matrai, P. A.: On the chemical dynamics of extracellular polysaccharides in the high Arctic surface microlayer, Ocean Sci., 8, 401–418, doi:10.5194/os-8-401-2012, 2012.

GESAMP: The sea-surface microlayer and its role in global change, in: Reports and Studies, WMO, 92, 1995.

Goldman, J. C., Dennett, M. R., and Frew, N. M.: Surfactant effects on air–sea gas exchange under turbulent conditions, Deep-Sea Res., 35, 1953–1970, doi:10.1016/0198-0149(88)90119-7, 1988.

Gutknecht, E., Dadou, I., Marchesiello, P., Cambon, G., Le Vu, B., Sudre, J., Garçon, V., Machu, E., Rixen, T., Kock, A., Flohr, A., Paulmier, A., and Lavik, G.: Nitrogen transfers off Walvis Bay: a 3-D coupled physical/biogeochemical modeling approach in the Namibian upwelling system, Biogeosciences, 10, 4117–4135, doi:10.5194/bg-10-4117-2013, 2013.

Harlay, J., De Bodt, C., Engel, A., Jansen, S., d'Hoop, Q., Piontek, J., Van Oostende, N., Groom, S., Sabbe, K., and Chou, L.: Abundance and size distribution of transparent exopolymer particles (TEP) in a coccolithophorid bloom in the northern Bay of Biscay, Deep-Sea Res. Pt. I, 56, 1251–1265, 2009.

Harvey, G. W. and Burzell, L. A.: A simple microlayer method for small samples, Limnol. Oceanogr., 11, 608–614, 1972.

Henrichs, S. M. and Williams, P. M.: Dissolved and particulate amino acids and carbohydrates in the sea surface microlayer, Mar. Chem., 17,141–163, 1985.

Hunter, K. A. and Liss, P. S.: Organic sea surface films, in: Marine Organic Chemistry, edited by: Duursma, E. K. and Dawson, R., Elsevier, Amsterdam, the Netherlands, 259–298, 1981.

Jähne, B. and Haußecker, H.: Air–water gas exchange, Annu. Rev. Fluid Mech., 30, 443–468, doi:10.1146/annurev.fluid.30.1.443, 1998.

Keeling, R. F., Körtzinger, A., and Gruber, N.: Ocean deoxygenation in a warming world, Ann. Rev. Mar. Sci., 2, 199–229, doi:10.1146/annurev.marine.010908.163855, 2010.

Keil, R. G. and Kirchman, D. L.: Bacterial hydrolysis of protein and methylated protein and its implications for studies of protein degradation in aquatic systems, Appl. Environ. Microb., 58, 1374–1375, 1992.

Kuznetsova, M. and Lee, C.: Enhanced extracellular enzymatic peptide hydrolysis in the sea-surface microlayer, Mar. Chem., 73, 319–332, 2001.

Kuznetsova, M. and Lee, C.: Dissolved free and combined amino acids in nearshore seawater, sea surface microlayers and foams: influence of extracellular hydrolysis, Aquat. Sci., 64, 252–268, doi:10.1007/s00027-002-8070-0, 2002.

Kuznetsova, M., Lee, C., Aller, J., and Frew, N. M.: Enrichment of amino acids in the sea-surface microlayers at coastal and open ocean sites in the North Atlantic Ocean, Limnol. Oceanogr., 49, 1605–1619, 2004.

Kuznetsova, M., Lee, C., and Aller, J.: Characterization of the proteinaceous matter in marine aerosols, Mar. Chem., 96, 359–377, doi:10.1016/j.marchem.2005.03.007, 2005.

Lachkar, Z. and Gruber, N.: What controls biological production in coastal upwelling systems? Insights from a comparative modeling study, Biogeosciences, 8, 2961–2976, doi:10.5194/bg-8-2961-2011, 2011.

Leck, C. and Bigg, E. K.: Source and evolution of the marine aerosol – a new perspective, Geophys. Res. Lett., 32, L19803, doi:10.1029/2005GL023651, 2005.

Lindroth, P. and Mopper, K.: High performance liquid chromatographic determination of subpicomole amounts of amino acids by precolumn fluorescence derivatization with o-phthaldialdehyde, Anal. Chem., 51, 1667–1674, 1979.

Liss, P. S.: Gas transfer: experiments and geochemical implications, in: Air–Sea Exchange of Gases and Particles, edited by: Liss, P. A. and Slinn, W. G., Nato asi series, Springer Netherlands, 241–298, 1983.

Liss, P. S. and Duce, R. A.: The Sea Surface and Global Change, Cambridge University Press, 2005.

Logan, B. E., Passow, U., Alldredge, A. L., Grossart, H.-P., and Simon, M.: Rapid formation and sedimentation of large aggregates is predictable from coagulation rates (half-lives) of transparent exopolymer particles (TEP), Deep-Sea Res. Pt. II, 42, 203–214, 1995.

Long, R. A. and Azam, F.: Abundant protein-containing particles in the sea, Aquat. Microb. Ecol., 10, 213–221, 1996.

Mari, X. and Burd, A.: Seasonal size spectra of transparent exopolymeric particles (TEP) in a coastal sea and comparision with those predicted using coagulation theory, Mar. Ecol.-Prog. Ser., 163, 63–76, 1998.

Mari, X. and Kiørboe, T.: Abundance, size distribution and bacterial colonization of transparent exopolymeric particles (TEP) during spring in the Kattegat, J. Plankton Res., 18, 969–986, 1996.

Matrai, P. A., Tranvik, L., Leck, C., and Knulst, J. C.: Are high Arctic surface microlayers a potential source of aerosol organic precursors?, Mar. Chem., 108, 109–122, 2008.

O'Dowd, C. D., Facchini, M. C., Cavalli, F., Ceburnis, D., Mircea, M., Decesari, S. Fuzzi, S., Yoon, Y. J., and Putaud, J.-P.: Biogenically driven organic contribution to marine aerosol, Nature, 431, 676–680, 2004.

Orellana, M. V., Matrai, P. A., Leck, C., Rauschenberg, C. D., Lee, A. M., and Coz, E.: Marine microgels as a source of cloud condensation nuclei in the high Arctic, P. Natl. Acad. Sci. USA, 108, 13612–13617, 2011.

Passow, U.: Transparent exopolymer particles (TEP) in aquatic environments, Prog. Oceanogr., 55, 287–333, 2002.

Paulmier, A. and Ruiz-Pino, D.: Oxygen minimum zones (omzs) in the modern ocean, Prog. Oceanogr., 80, 113–128, doi:10.1016/j.pocean.2008.08.001, 2009.

Paulmier, A., Ruiz-Pino, D., and Garcon, V.: The oxygen minimum zone (omz) off Chile as intense source of CO_2 and N_2O, Cont. Shelf Res., 28, 2746–2756, doi:10.1016/j.csr.2008.09.012, 2008.

Paulmier, A., Ruiz-Pino, D., and Garçon, V.: CO_2 maximum in the oxygen minimum zone (OMZ), Biogeosciences, 8, 239–252, doi:10.5194/bg-8-239-2011, 2011.

Prieto, L., Ruiz, J., Echevarria, F., Garcia, C. M., Bartual, A., Galvez, J. A., Corzo, A., and Macias, D.: Scales and processes in the aggregation of diatom blooms: high time resolution and wide size range records in a mesocosm study, Deep-Sea Res. Pt. I, 49, 1233–1253, 2002.

Quinn, P. K. and Bates, T. S.: The case against climate regulation via oceanic phytoplankton sulphur emissions, Nature, 480, 51–56, 2011.

Quinn, P. K., Bates, T. S., Schulz, K. S., Coffman, D. J., Frossard, A. A., Russell, L. M., Keene, W. C., and Kieber, D. J.: Contribution of sea surface carbon pool to organic matter enrichment in sea spray aerosol, Nat. Geosci., 7, 228–232, doi:10.1038/ngeo2092, 2014.

Reinthaler, T., Sintes, E., and Herndl, G.: Dissolved organic matter and bacterial production and respiration in the sea-surface microlayer of the open Atlantic and the western Mediterranean Sea, Limnol. Oceanogr., 53, 122–136, 2008.

Riebesell, U., Körtzinger, A., and Oschlies, A.: Sensitivities of marine carbon fluxes to ocean change, P. Natl. Acad. Sci. USA, 106, 20602–20609, 2009.

Russell, L. M., Hawkins, L. N., Frossard, A. A., Quinn, P. K., and Bates, T. S.: Carbohydrate-like composition of submicron atmospheric particles and their production from ocean bubble bursting, P. Natl. Acad. Sci. USA, 107, 6652–6657, 2010.

Salter, M. E., Upstill-Goddard, R. C., Nightingale, P. D., Archer, S. D., Blomquist, B., Ho, D. T., Huebert, B., Schlosser, P., and Yang, M.: Impact of an artificial surfactant release on air–sea gas fluxes during Deep Ocean Gas Exchange Experiment II, J. Geophys. Res.-Oceans, 116, C11016, doi:10.1029/2011JC007023, 2011.

Santos, A. L., Oliveira, V., Baptista, I., Henriques, I., Gomes, N. C., Almeida, A., Correia, A., and Cunha, A.: Effects of UV-B radiation on the structural and physiological diversity of bacterioneuston and bacterioplankton, Appl. Environ. Microb., 78, 2066–2069, doi:10.1128/aem.06344-11, 2012.

Schlitzer, R.: Ocean Data View, available at: http://odv.awi.de (last access: March 2015), 2013.

Schulz, K. G., Bellerby, R. G. J., Brussaard, C. P. D., Büdenbender, J., Czerny, J., Engel, A., Fischer, M., Koch-Klavsen, S., Krug, S. A., Lischka, S., Ludwig, A., Meyerhöfer, M., Nondal, G., Silyakova, A., Stuhr, A., and Riebesell, U.: Temporal biomass dynamics of an Arctic plankton bloom in response to increasing levels of atmospheric carbon dioxide, Biogeosciences, 10, 161–180, doi:10.5194/bg-10-161-2013, 2013.

Solomon, S., Qin, D., Manning, M., Chen, Z., Marquis, M., Averyt, K. B., Tignor, M., and Miller, H. L.: Climate Change 2007: the Physical Science Basis. Contribution of Working Group I to the Fourth Assessment Report of the Intergovernmental Panel on Climate Change, Cambridge University Press, Cambridge, UK, New York, NY, USA, 2007.

Stramma, L., Johnson, G. C., Sprintall, J., and Mohrholz, V.: Expanding oxygen-minimum zones in the tropical oceans, Science, 320, 655–658, doi:10.1126/science.1153847, 2008.

Stolle, C., Nagel, K., Labrenz, M., and Jürgens, K.: Succession of the sea-surface microlayer in the coastal Baltic Sea under natural and experimentally induced low-wind conditions, Biogeosciences, 7, 2975–2988, doi:10.5194/bg-7-2975-2010, 2010.

Sugimura, Y. and Suzuki, Y.: A high-temperature catalytic oxidation method for the determination of non-volatile dissolved organic carbon in seawater by direct injection of a liquid sample, Mar. Chem., 24, 105–131, doi:10.1016/0304-4203(88)90043-6, 1988.

Tarazona, J. and Arntz, W.: The Peruvian coastal upwelling system, in: Coastal Marine Ecosystems of Latin America, edited by: Seeliger, U. and and Kjerfve, B., Springer, Berlin, Heidelberg, Germany, 229–244, 2001.

Upstill-Goddard, R. C.: Air–sea gas exchange in the coastal zone, Estuar. Coast. Shelf S., 70, 388–404, doi:10.1016/j.ecss.2006.05.043, 2006.

Upstill-Goddard, R. C., Frost, T., Henry, G. R., Franklin, M., Murrell, J. C., and Owens, N. J. P.: Bacterioneuston control of air–water methane exchange determined with a laboratory gas exchange tank, Global Biogeochem. Cy., 17, 1108, doi:10.1029/2003gb002043, 2003.

van Pinxteren, M., Müller, C., Iinuma, Y., Stolle, C., and Herrmann, H.: Chemical characterization of dissolved organic compounds from coastal sea surface microlayers (Baltic Sea, Germany), Environ. Sci. Technol., 46, 10455–10462, doi:10.1021/es204492b, 2012.

Verdugo, P., Alldredge, A. L., Azam, F., Kirchman, D. L., Passow, U., and Santschi, P. H.: The oceanic gel phase: a bridge in the DOM–POM continuum, Mar. Chem., 92, 67–85, 2004.

Wallace, G. T. and Duce, R. A.: Transport of particulate organic matter by bubbles in marine waters 1, Limnol. Oceanogr., 23, 1155–1167, doi:10.4319/lo.1978.23.6.1155, 1978.

Wurl, O., Miller, L., Röttgers, R., and Vagle, S.: The distribution and fate of surface-active substances in the sea-surface microlayer and water column, Mar. Chem., 115, 1–9, 2009.

Wurl, O., Miller, L., and Vagle, S.: Production and fate of transparent exopolymer particles in the ocean, J. Geophys. Res., 116, C00H13, doi:10.1029/2011JC007342, 2011.

Zhou, J., Mopper, K., and Passow, U.: The role of surface-active carbohydrates in the formation of transparent exopolymer particles by bubble adsorption of seawater, Limnol. Oceanogr., 43, 1860–1871, 1998.

Table 1. Hydrographic conditions encountered during SML sampling off Peru in 2012 (M91).

	Temperature (˚C)	Salinity	Air temperature (˚C)	Wind speed ($\mathrm{m\,s^{-1}}$)	Global Radiation ($\mathrm{W\,m^{-2}}$)	UV Radiation ($\mathrm{W\,m^{-2}}$)
average	19.25	34.87	19.67	5.66	570	37 935
SD	1.70	0.50	0.89	2.14	366	23 384
Min	15.91	32.02	17.30	0.60	10	0.812
Max	21.90	35.32	21.50	9.00	1103	71.10

Title Page
Abstract Introduction
Conclusions References
Tables Figures
◀| |▶
◀ ▶
Back Close
Full Screen / Esc
Printer-friendly Version
Interactive Discussion

Table 2. Concentration of various organic components in the SML during M91, given as average (avg.) and standard deviation (SD), as well as minimum (min) and maximum (max); *n*: number of observations.

	Unit	Avg.	SD	min	max	*n*
DOC	$\mu mol\,L^{-1}$	94	13	71	122	39
TOC	$\mu mol\,L^{-1}$	127	33	82	199	39
POC	$\mu mol\,L^{-1}$	33	25	2.3	96	39
TEP number	$\times 10^6\,L^{-1}$	19	15	1.8	63	39
TEP area	$mm^2\,L^{-1}$	100	106	6.9	408	39
DCCHO	$nmol\,L^{-1}$	1111	550	507	2668	39
PCCHO	$nmol\,L^{-1}$	1084	1300	41	5156	34
TN	$\mu mol\,L^{-1}$	16	4.9	8.7	28	39
TDN	$\mu mol\,L^{-1}$	12.5	4.0	7.7	25	39
PN	$\mu mol\,L^{-1}$	3.3	3.7	bd	16	39
CSP number	$\times 10^6\,L^{-1}$	118	72	19	311	39
CSP area	$mm^2\,L^{-1}$	1024	728	137	3051	39
FAA	$nmol\,L^{-1}$	151	104	49	531	37
DHAA	$nmol\,L^{-1}$	770	359	423	2017	30
PHAA	$nmol\,L^{-1}$	1176	774	208	3956	29
bacteria	$\times 10^3\,mL^{-1}$	1955	2057	30	8538	36
phytoplankton	$\times 10^3\,mL^{-1}$	45	53	5.4	300	35

Table 3. Correlation coefficients between concentrations of various organic components in the SML and their concentration in the underlying seawater (xULW), temperature (T, °C), and wind speed (U, $\mathrm{m\,s^{-1}}$). Correlations yielding significance level of $p < 0.01$ are marked bold.

SML	xULW	T	U
DOC	**0.75**	−0.04	0.06
TOC	**0.79**	**−0.53**	−0.35
POC	**0.68**	**−0.67**	**−0.48**
TEP number	**0.51**	**−0.58**	**−0.69**
TEP area	**0.58**	**−0.65**	**−0.69**
DCCHO	**0.94**	**−0.44**	−0.29
PCCHO	**0.77**	**−0.59**	**−0.38**
TDN	0.24	−0.18	−0.05
PN	**0.59**	**−0.55**	**−0.43**
CSP number	**0.53**	−0.04	0.15
CSP area	**0.68**	−0.36	−0.31
FAA	0.34	−0.34	0.19
DHAA	0.30	**−0.47**	−0.37
PHAA	**0.56**	**−0.64**	**−0.53**

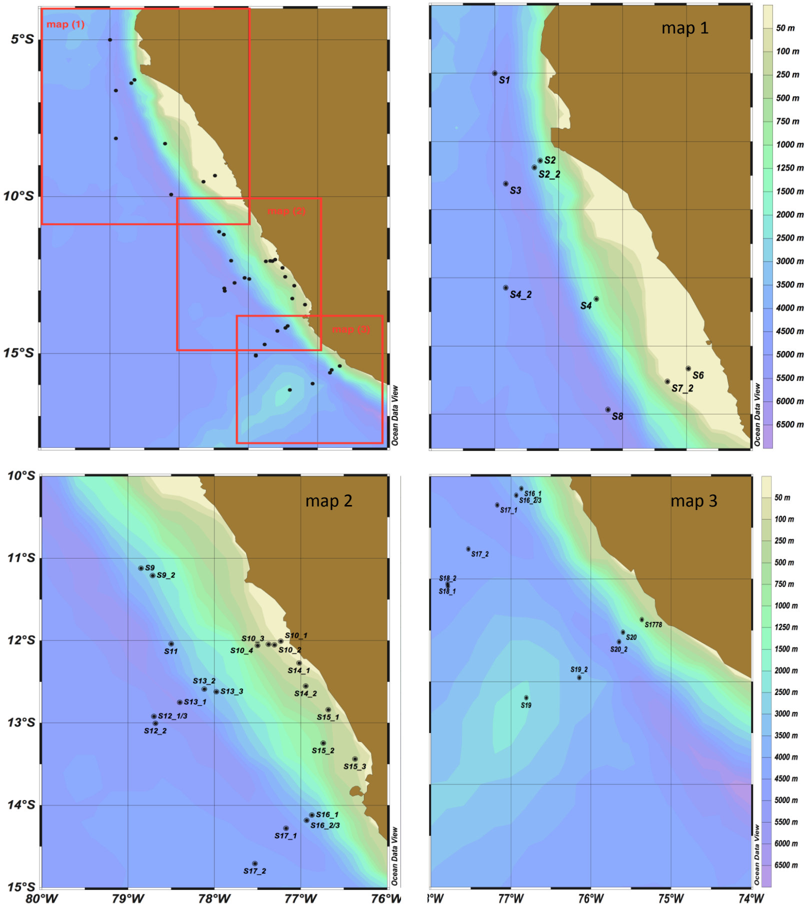

Figure 1. Maps of stations where sampling for sea surface microlayer (SML) and underlying seawater (ULW) was conducted during the SOPRAN Meteor 91 cruise along the coastal upwelling area off Peru in 2012.

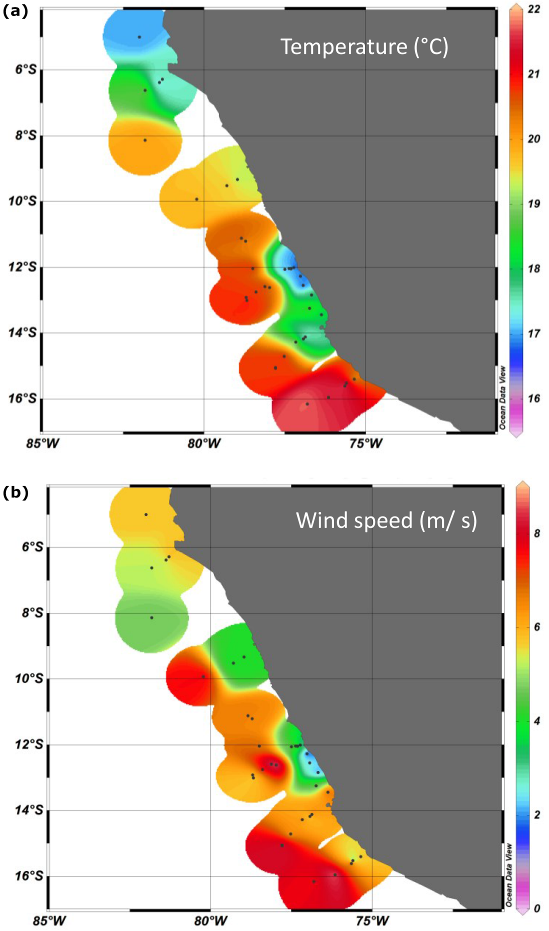

Figure 2. (a, b) Surface water (1 m depth) temperature (°C) **(a)** and wind speed ($\mathrm{m\,s^{-1}}$) **(b)** during M91.

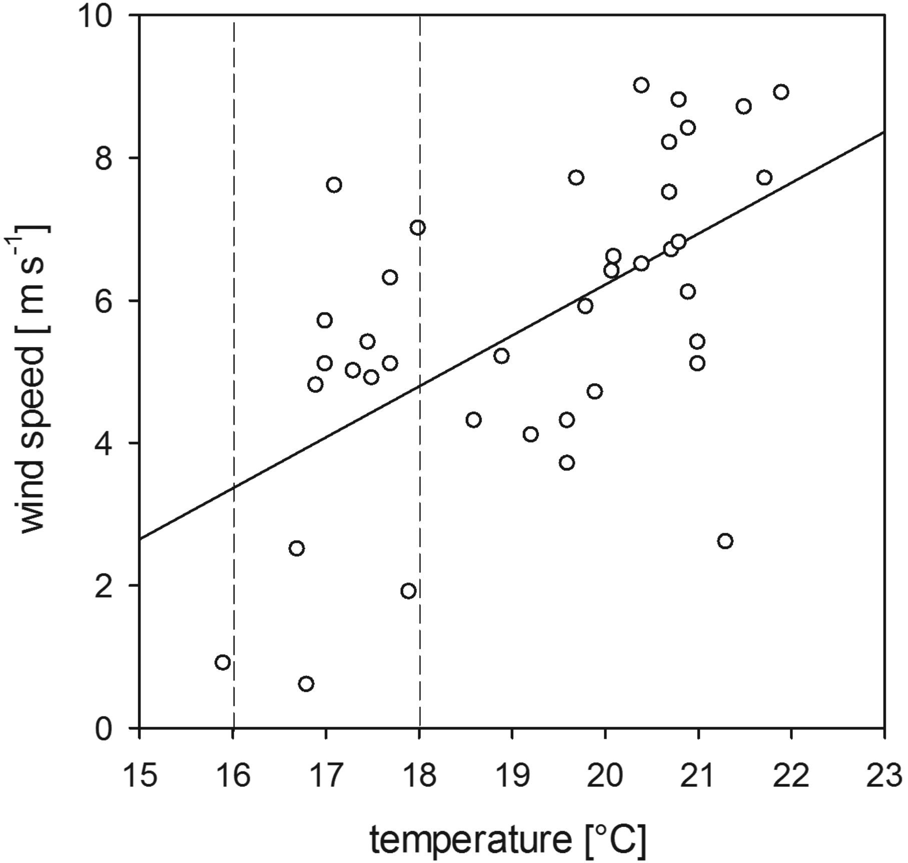

Figure 3. Direct relationship between surface water temperature and wind speed during M91 SML sampling, $p < 0.001$, $r = 0.58$, $n = 39$. Data in dotted rectangles were selected for analysis of wind speed effects at similar temperatures, see Fig. 7.

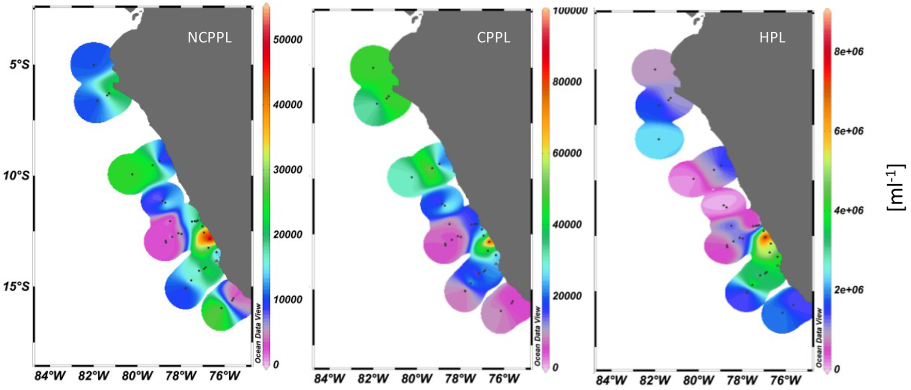

Figure 4. Phyto- and bacterioneuston abundance (number mL^{-1}) in the SML off Peru during M91: NCPPL: "Non-cyanobacterial-type" picophytoplankton, CPPL: "cyanobacterial-type" picophytoplankton, HPL: heterotrophic picoplankton.

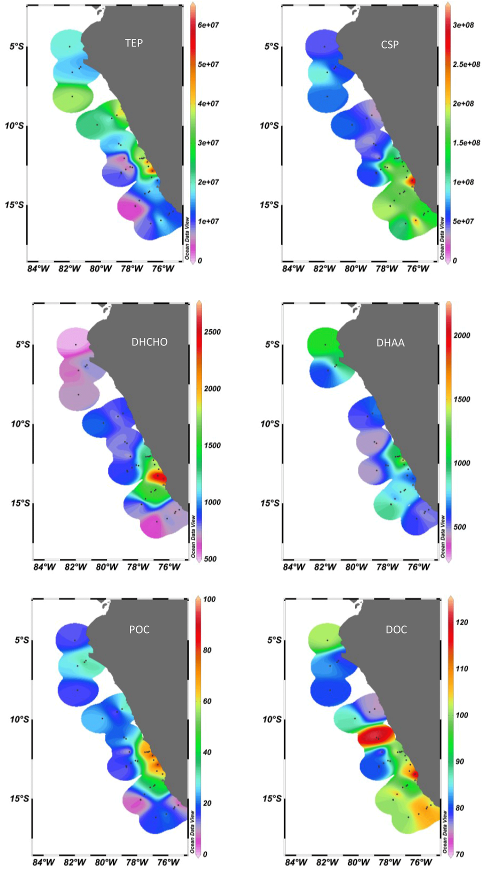

Figure 5. Surface distribution patterns of organic matter concentrations in the SML during M91 showing particulate organic carbon (POC, µmol L^{-1}), dissolved organic carbon (DOC, µmol L^{-1}) dissolved hydrolysable carbohydrates (DHCHO, nmol L^{-1}), dissolved hydrolysable amino acids (DHAA, nmol L^{-1}) and abundance of TEP (L^{-1}) and CSP (L^{-1}).

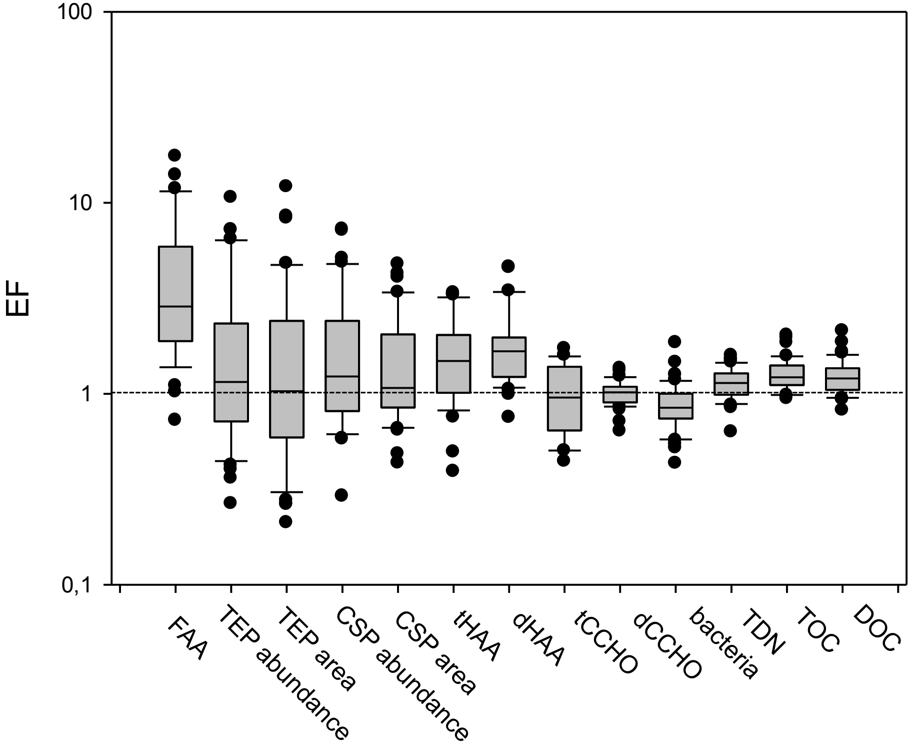

Figure 6. Box and whisker plot of enrichment factors (EF) calculated for various particulate and dissolved components during M91. Each box encloses 50 % of the data with the median value of the variable displayed as a line. The bottom of the box marks the 25 %, and the top the 75 % limit of data. The lines extending from the top and bottom of each box mark the 10 and 90 % percentiles within the data set and the filled circles indicate the data outside of this range.

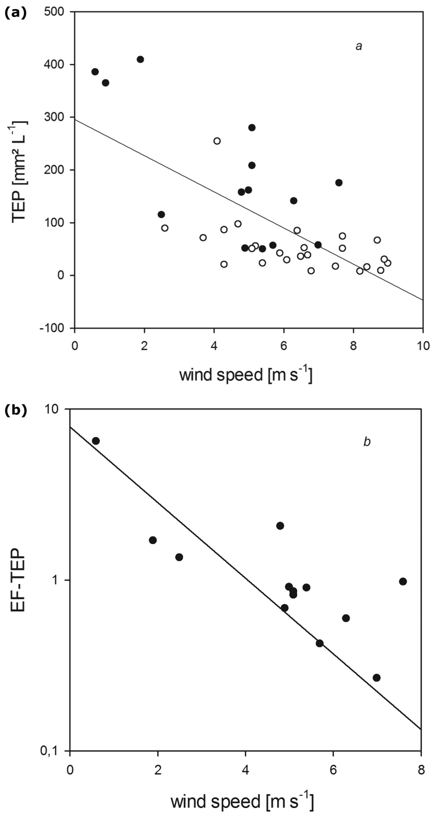

Figure 7. (a, b) Influence of wind speed ($\mathrm{m\,s^{-1}}$) on the total area concentration of TEP ($\mathrm{mm^2\,L^{-1}}$) in the SML **(a)** and relationship between TEP enrichment factors (EF) and wind speed ($\mathrm{m\,s^{-1}}$) for stations of similar sea surface temperature as indicate in Fig. 3. **(b)** Filled dots indicated data from stations of similar sea surface temperature.

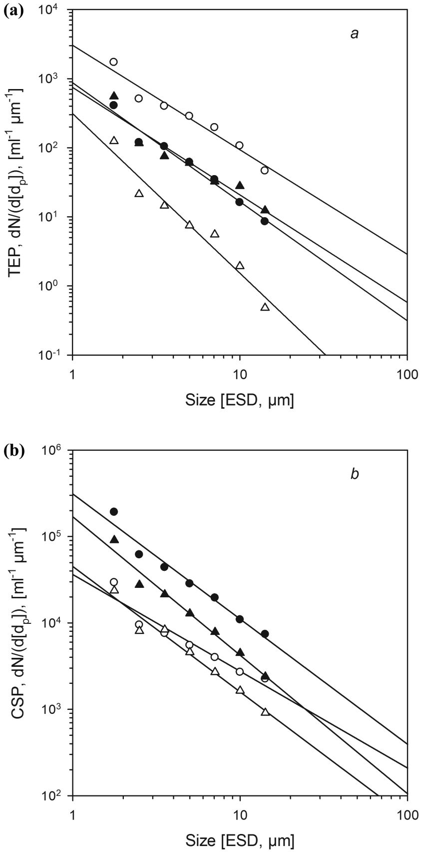

Figure 8. (a, b) Size frequency distribution of TEP **(a)** and CSP **(b)** observed during the M91 cruise for samples collected from the SML (open symbols) and in the ULW (filled symbols) at the stations with lowest wind speed of 0.6 m s^{-1} (circles) and highest wind speed of 9.0 m s^{-1} (triangles). Linear regression of log(dN/d(d_p)) vs. log(d_p) was fitted to the particles in the size range of 1.05–14.14 µm ESD.

Title Page
Abstract Introduction
Conclusions References
Tables Figures
|◀ ▶|
◀ ▶
Back Close
Full Screen / Esc
Printer-friendly Version
Interactive Discussion